ELSEVIER

Open Zn-URJC-13 efficient catalyst for mild CO_2 transformation using bulky epoxides

Jesús Tapiador [*], Pedro Leo, Guillermo Calleja, Gisela Orcajo

Chemical and Environmental Engineering Group, ESCET, Universidad Rey Juan Carlos, c/Tulipán s/n 28933 Móstoles, Spain

ARTICLE INFO

ABSTRACT

In CO_2 cycloaddition reactions with epoxides that have bulky or long-chain substituents, the yield significantly decreases when using heterogeneous catalysts, including MOFs, with micropores smaller than 14 Å. In this study, a new MOF material called Zn-URJC-13 is reported. This MOF combines different features such as that it contains acid and basic Lewis sites based on Zn and -NH$_2$ groups, exhibits permanent porosity with a bimodal porous system centered at 11 and 17 Å suitable for the diffusion of cycloaddition reaction species, and it is chemically stable in various common organic solvents. The aim of this material is to improve the textural properties of other MOFs with similar chemical compositions, making it suitable as a catalyst for CO_2 cycloaddition reactions with epoxides even bulky. This novel material exhibits high affinity to CO_2 molecules, with a Q_{st} of 62 kJ/mol. The Zn-URJC-13 catalyst demonstrates efficient performance in CO_2 cycloaddition reactions using a wide range of epoxides, including those with long-chain and bulky substituents such as allyl glycidyl ether and styrene oxide. It can achieve an epoxide conversion as high as 84 % and selectivity to carbonate products above 90 % for the bulkiest styrene oxide. When compared to other Zn-based MOF materials with similar or different structures but without amino groups, the new material exhibits superior catalytic performance. Furthermore, Zn-URJC-13 can be reused in five consecutive reaction cycles while maintaining its efficient catalytic behavior and crystalline structure. These findings highlight the notable potential of Zn-URJC-13 for CO_2 cycloaddition transformation routes.

1. Introduction

Due to their considerable impact on climate change and the environment, carbon dioxide (CO_2) emissions have risen to the top of the list of urgent global concerns [1]. The persistent growth in atmospheric CO_2 concentrations is mostly attributable to human activities like burning fossil fuels and deforestation [2,3]. Increasing global temperatures, increasing sea levels, and ecosystem disruptions have all been connected to this increase in CO_2 levels [4].

A potential action to the twin challenges of reducing CO_2 emissions and creating sustainable carbon-based products is the carbon dioxide valorization [2,4]. Carbon Capture and Utilization (CCU) systems involve removing carbon dioxide from ambient air or industrial exhaust gases and turning it into valuable products [5]. For the conversion of CO_2 into chemicals, fuels, and materials, a variety of transformation routes, including catalytic, electrochemical and biological conversion have been reported in the literature with great conversion results [6].

The synthesis of cyclic carbonates through the catalytic cycloaddition reaction between carbon dioxide and epoxides has gained significant attention in the field of green chemistry [7,8]. Different industries use cyclic carbonates for a variety of purposes. They act as crucial intermediates in the synthesis of polycarbonates, which are widely used to make adhesives, coatings, and plastics [7,9]. Due to their excellent ionic conductivity and stability, cyclic carbonates can be also used as electrolytes in energy storage systems like lithium-ion batteries and supercapacitors [9]. In the pharmaceutical and chemical sectors, cyclic carbonates are also used as solvents, blowing agents, and chemical feedstocks [7]. However, in terms of achieving high reaction yields and selectivity and reusable catalysts, it needs to be improved [9].

Metal-Organic Frameworks (MOFs) are a class of versatile materials with a variety of properties. They are being tested in wide range of applications, including gas storage, catalysis, energy storage, sensing, and environmental remediation, due to their configurable architectures, high porosity, and adaptable qualities [10]. These characteristics make them potential catalysts in cycloaddition reaction between CO_2 [11,12], and in particular, they can contain in their structures basic and acid

Lewis center that play key roles in the cycloaddition reaction between CO_2 and epoxides [13,14].

Different MOF materials constituted by metal clusters or centers such as Mg^{2+}, Mn^{2+}, Co^{2+}, Ni^{2+}, Cu^{2+} and Zn^{2+} have been reported to be used as catalysts in this reaction [15,16]. It has been observed that Zn^{2+} metal ion in MOFs presents the best catalytic performance since the suitable Lewis acid properties of the metal [17]. Besides, the presence of functional organic groups with free electrons pairs, performing as basic Lewis sites, such as amine groups, can also enhance the yield of the reaction due to its activation effect over the CO_2 molecules [18,19,43]. However, when epoxides with bulky substituents are used in the reaction, apart from the presence of acid and basic Lewis sites, it is also influencing the porous system of the heterogeneous catalyst to avoid diffusional hindrances of reactants and products [20].

Bian et al. [21] synthesized a new MOF material BUT-127 constituted by two different organic ligands (1,4-benzenediprazole and isophthalic acid with different substituent) and Co^{2+} as metal center. BUT-127 material shown a high propylene oxide conversion of 95 % under 1 bar of CO_2, using 99 mg of TBAB as co-catalyst under room temperature for 48 h. Nonetheless, when the epoxide used was butylene oxide the conversion decreased to 65 % due to the steric hindrance produced inside the porous system of the material. Another MOF used as catalyst in cycloaddition reaction was CuAspBix synthesized by Kathalikkattil et al. [22]. This material achieved a high epoxide conversion of 92 % when epichlorohydrin was used as substrate, but 61 % for styrene oxide under elevated temperature of 100 °C, 12 bar of carbon dioxide using 13 mg of TBAB as co-catalyst for 12 h. Dhankhar et al. reported a new MOF ($Tb_2(ImBDC)_3(H_2O)_2$) constituted by 2-(imidazole-1-yl)terephthalic acid and Tb^{3+} as metal center that converted 99 % of epichlorohydrin [23], however, when styrene oxide and 1,2-epoxyhexadecane were used, the epoxide conversion decreased to 32 % and 25 %, respectively, due to the strong diffusional constraints generated in the cavities of the material. Based on these examples, it is clear that textural properties play and important role in this reaction when bulky epoxides are used, which is in agreement with Kim et al. [24].

Herein, a new MOF material, based on acid zinc ions, basic amino groups, hydrophobic pyridine is evaluated and compared to other heterogeneous catalysts in terms of textural properties and chemical nature in the CO_2 cycloaddition reaction using epoxides with bulky substituents, such as styrene oxide. Additionally, the synthesis of this material is cheaper than many reported MOFs due to the organic ligands present in the Zn-URJC-13 are commercially available with a reduced cost.

2. Experimental section

2.1. Materials and measurements

All starting materials and solvents were purchased from Cymit Química S.L. and used without further purification.

2.2. Synthesis of Zn-URJC-13

0.05 mmol (0.012 g) of biphenyl-4,4′-dicarboxylic acid, 0.1 mmol (0.014 g) of 2-aminopyridine-4-carboxylic acid and 0.1 mmol (0.030 g) of $Zn(NO_3)_2$ were mixed in 5 ml of DMF. The yellow-colored suspension was sonicated for 10 min and then heated at 100 °C for 72 h. After this time, yellow crystals were separated by filtration, washed three times with DMF and dried in air. Yield: 68 % based on metal center. Elemental analysis (%) calculated: C, 49.16; H, 3.42; N, 5.68. Found (%): C, 50.21; H, 3.37; N, 5.86. FT-IR: 3421 (w), 3348 (w), 3068 (w), 2929 (w), 2860 (w), 2802 (w), 1658 (s), 1628 (sh), 1605 (s), 1550 (m), 1495 (w), 1460 (w), 1384 (s), 1324 (sh), 1254 (m), 1177 (m), 1092 (m), 1062 (w), 1021 (sh), 1005 (m), 846 (m), 839 (m), 771 (s), 677 (w) and 660 (w) cm^{-1}.

2.3. Physicochemical characterization techniques

Powder X-ray diffraction (PXRD) patterns were obtained in a Philips XPERT PRO (URJC, Móstoles, Spain), and with a Bruker d8 equipped with a position sensitive detector (X-ray diffraction facility, ICMM), using CuKα (λ = 1.542 Å) radiation. In all the cases the sample were grounded to reduce the effects of preferred crystal orientation. Structural analysis including Rietveld refinement was completed with BIOVIA Materials Studio 2021 software package. Crystallographic data for the reported structure has been deposited in the Cambridge Crystallographic Data Center as supplementary publication no. CCDC 2281588. Additional crystal data are shown in section S1. Copies of the data can be obtained free of charge at http://www.ccdc.cam.ac.uk/products/csd/request. ^1H NMR spectra were collected with a Varian Mercury Plus spectrometer at 400 MHz using trimethyl silane as an internal standard. FID files were processed using MestRe-C software version 4.9.9.6. The chemical shifts (δ) for ^1H spectra, given in ppm, are referenced to the residual proton signal of the deuterated solvent. Fourier transform-infrared spectra (FT-IR) were recorded for powder samples in a Varian 3100 Excalibur Series spectrometer (URJC, Móstoles, Spain) with a resolution of 4 cm^{-1}. Thermogravimetric analyses (TGA) were carried out under air atmosphere in a Mettler-Toledo DSC-TGA Star System device. Scanning electron microscopy (SEM) images and EDS analysis were obtained on a TM1000-Hitachi operated at 15 kV. Argon adsorption-desorption isotherms were measured at 87 K on an 3Flex Surface Analyzer (Micromeritics, URJC, Móstoles, Spain). The specific surface area was calculated by the Brunauer-Emmett-Teller (BET) equation [25].

2.4. Adsorption/desorption isotherms of pure CO_2 and isosteric heat of adsorption

Adsorption/desorption isotherms of pure CO_2 were collected in a volumetric analyzer type VTI HPVA-100 Scientific Instrument. Approximately 110 mg of Zn-URJC-13 were previously evacuated in-situ under vacuum ($9 \cdot 10^{-3}$ bar) at 110 °C for 12 h, and then cooled down up to the analysis temperature using a thermostatic polyethyleneglycol bath. Isotherm equilibrium points were collected considering the following two equilibrium criteria: i) a pressure drop below 0.2 mbar in 3 min or ii) a maximum equilibrium time of 60 min. CO_2 adsorption equilibrium points at 25 and 45 °C were fitted to Sips equation (Sips, 1948). The Clausius-Clapeyron equation was used to determine the isosteric heat of adsorption profile from the slope of the best linear fit of ln(P) versus (1/T) at each CO_2 loading (additional details are included in S3).

2.5. Catalytic test of Zn-URJC-13 in the cycloaddition of CO_2 and epoxides at mild conditions

For catalytic test, Zn-URJC-13 was degassed at 150 °C for 12 h. In a model experiment, 1 mmol of epoxide, 1–2 mol % of degassed MOF catalyst (Zn to epoxide ratio) and 4–6 mol % of co-catalyst (tetrabutylammonium bromide, TBAB) (TBAB to epoxide ratio) were added in a 100 ml stainless-steel autoclave. The system was evacuated with CO_2 three times before being pressurized at different CO_2 pressures (see Table 1). Then, the reaction was carried out at room temperature under moderate stirring. Once the reaction time was completed, the residual carbon dioxide was slowly discharged, and the catalyst was separated by centrifugation. To determine the conversion of epoxide and selectivity to cyclic carbonate, the products were analyzed by 1 H NMR using $CDCl_3$ as solvent and 1, 2, 4, 5-tetrachloro-3-nitrobenzene as internal standard (Sections S4 and S5 of Supporting information).

Table 1
Reaction conditions study of CO_2 cycloaddition with epichlorohydrin.

Entry	Catalyst (%)	Co-catalyst (%)	P (bar)	Time (h)	Conv. (%)[a]	Sel. (%)[b]
1	0	5	12	24	39	
2	1.5	0	12	24	3	
3	1	5	12	24	93	
4	1.5	5	12	24	98	
5	2	5	12	24	88	
6	1.5	4	12	24	86	>99
7	1.5	6	12	24	98	
8	1.5	5	6	24	67	
9	1.5	5	1	24	47	
10	1.5	5	12	12	57	
11	1.5	5	12	6	44	

[a,b]Determinated by H NMR.

3. Results and discussion

3.1. Catalyst characterization

From the organic ligands 2-aminopyridine-4-carboxylic acid (or 2-aminoisonicotinic acid) and 4,4′-biphenyldicarboxylic acid, and zinc nitrate as metal source, the synthesis of the material Zn-URJC-13 has been carried out. The material was crystallized by a solvothermal process using 5 ml of DMF as solvent and a Zn^{2+}/2-aminoisonicotinic/4,4′-biphenyldicarboxylic acid ratio of 1/1/1, at 130 °C for 72 h. Under these synthesis conditions, yellow plate-shaped crystals were obtained which were characterized by the following techniques.

X-ray single crystal diffraction analysis on compound Zn-URJC-13 shows that it crystallizes with the $[Zn_2(4,4′\text{-}BPDC)(NH_2\text{-}ISNC)_2]\cdot DMF$ chemical formula in the orthorhombic $Pmc2_1$ space group. The asymmetric unit of this new material is constituted by two different Zinc(II) atoms coordinated to tree oxygen atoms of carboxylate groups, one of them from the organic ligand 4,4′-byphenyldicarboxilic acid and the others from the two different 2-aminoisonicotinic acid. The metallic cluster $Zn_2N_2O_8$ (Fig. 1) is constituted by eight oxygen atoms, four of them from carboxylate group of the organic ligand 4,4′-byphenyldicarboxilic acid and four from the carboxylate group of 2-aminoisonicotinic acid, and two nitrogen atoms from pyridinic organic ligand in axial position (not shown). The simulated and experimental patterns are showed in Fig. S2.1.

The distances of Zn-O are in the range of 1.93–2.34 Å and the distances Zn-N and Zn-Zn are 1.97 and 2.97 Å, respectively. The crystalline structure of Zn-URJC-13 generates different channels along the crystallographic axes *a*, *b* and *c* (Fig. 2). The channels along *a* axis have an average size of 11,5 Å (not shown), meanwhile the channels along *c* axis around 15,0 Å (Fig. 2).

By means of infrared spectroscopy the presence of the main functional groups of both organic ligands was verified. Fig. 3 shows the infrared spectrum where the ν(N-H) vibration bands of the -NH_2 group
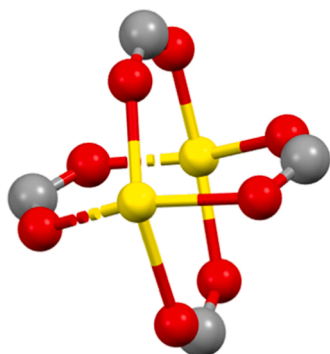
of the 2-aminoisonicotinic acid ligand are identified at 3429 and 3350 cm^{-1}, and the ν(N = C) vibration band at 1607 cm^{-1} of this same organic ligand is also observed. On the other hand, the ν_a(C=O) vibration band of carboxylic acids at 1658 cm^{-1} is also showed.

To determine the thermal stability of the new material, a thermogravimetric analysis (TGA) was performed in oxidizing atmosphere (Fig. S2.2). As can be seen, this material has two clearly marked mass losses, the first one of 20 %, from 40° to 150°C, corresponding to the loss of DMF retained in the pores of the material and the second one at 400 °C corresponding to the degradation of the organic ligands, causing the collapse of the structure. Before the measurement of textural properties, the Zn-URJC-13 material was degassed at a temperature of 150 °C and at high vacuum for 12 h. After degassing, it was again characterized by TGA to check the removal of the solvent retained in the pores. As shown in Fig. S2.2, under these degassing conditions, the removal of the DMF adsorbed on the material is achieved. In addition, the powder XRD diffractogram of the degassed material was recorded to confirm that it was stable after the activation process (Fig. S2.3).

The textural properties were measured by Ar adsorption/desorption isotherms at 87 K (Fig. 4). The Zn-URJC-13 material presents a Type I isotherm characteristic of microporous materials according to the IUPAC classification [26] where a sharp rise in adsorption branch at low pressures is produced; in addition, both the positive slope and the small hysteresis loop demonstrate the presence of larger pores. The data analysis gave a specific surface area of 397 m^2/g, a pore volume of 0.325 cm^3/g and a pore size distribution (shown in Fig. S2.4) that demonstrates that the new material has a bimodal distribution centered at 11 and 17 Å, which agrees with the crystallographic data.

The crystals of this material have a rectangular morphology with an average crystal size of 500 μm, as seen in the SEM images in Fig. 5.

Once the stability of this new MOF material was verified after the degassing process, CO_2 adsorption isotherms were carried out at 25 and 45 °C at 6 bar CO_2 pressure (Fig. 6). The Zn-URJC-13 material showed a CO_2 adsorption capacity of 2.95 and 2.39 mmol/g at 25 and 45 °C and 6 bar, respectively, which are higher than most of the MOF materials studied in the literature [27]. Another very interesting aspect is that in both isotherms a hysteresis cycle, typical of a chemisorption process, is observed [28–30], which is corroborated by a high heat of CO_2 adsorption estimated at low coverage of 62 kJ/mol. The complete Q_{st} profile is shown in Fig. S3.1.

The CO_2 heat of adsorption at low coverage of the Zn-URJC-13 material surpassed those of other MOF materials with NH_2 groups in their structure such as Cu-URJC-8 [18,19] or NH_2-MIL-53 [31], indicating the stronger CO_2 interaction with this structure. This behavior could not be only due to the proximity between the amino groups of the 2-aminopyridine-4-carboxylic acid ligand, but also because of the CO_2 confinement effect produced in its smaller cavities of 11 Å due to the van der Waals additional forces, which thermodynamically favors the formation of carbamate groups from carbon dioxide, as Planas et. al have proposed in their work [32].

3.2. Cycloaddition reaction with carbon dioxide and epoxides

Firstly, motivated by the great affinity of the new MOF to CO_2 molecules, Zn-URJC-13 was evaluated in the cycloaddition reaction between CO_2 and epichlorohydrin, which is a small epoxide that should not produce any diffusional restrictions, so the accessibility to the active sites is complete. To find the economically and environmentally best reaction conditions using Zn-URJC-13, these variables were studied: amount of catalyst and co-catalyst (tetrabutylammonium bromide -TBAB), CO_2 pressure and reaction time. The reaction conditions and results are summarized in Table 1.

The conversion of epichlorohydrin without catalyst was 39 % (entry 1). TBAB can open the epoxide ring by the presence of bromide ion generated in the reaction medium. Without co-catalyst the reaction result was 3 % due to the MOF material cannot open the ring of epoxide

Fig. 1. Metallic cluster of Zn-URJC-13. O: red, C: grey, Zn: yellow, N: light blue.
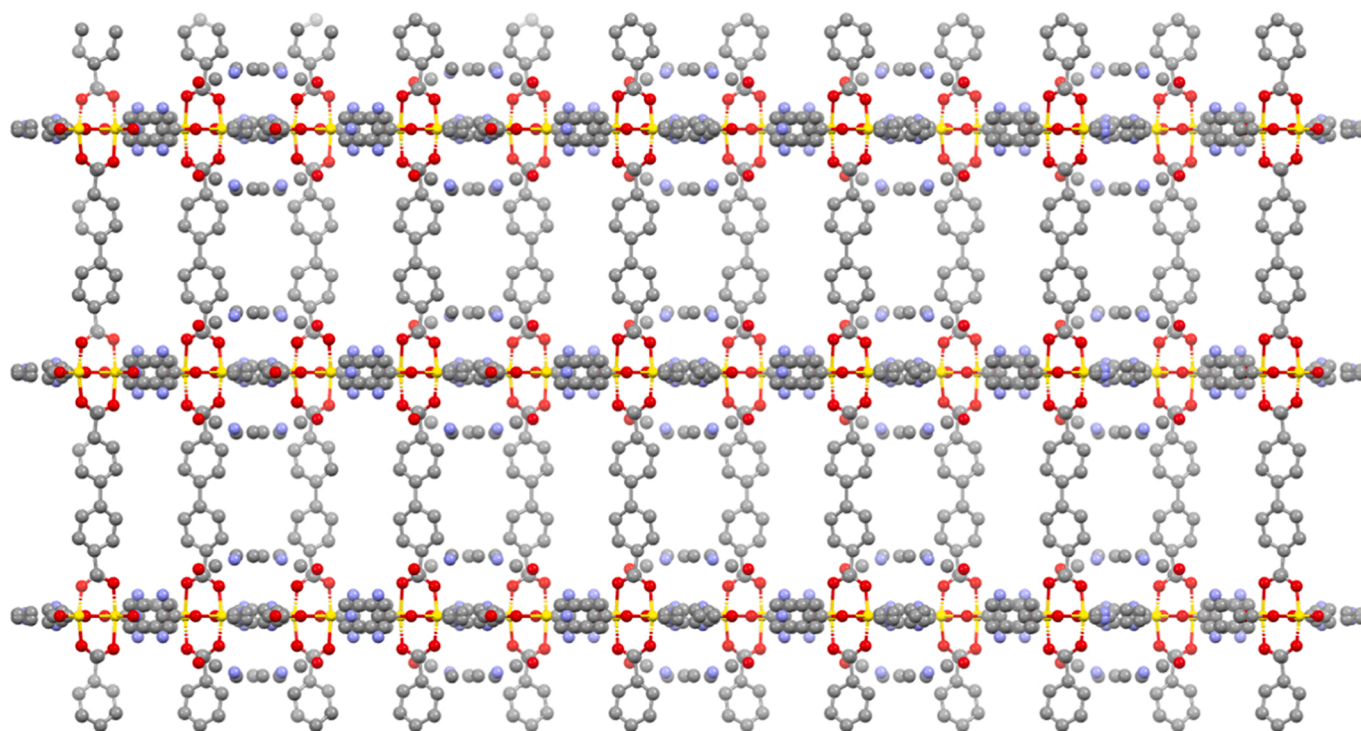
Fig. 2. Mercury perspective of Zn-URJC-13 Metal-Organic Framework along the crystallographic axis *c*. O: red, C: grey, Zn: yellow, N: light blue.
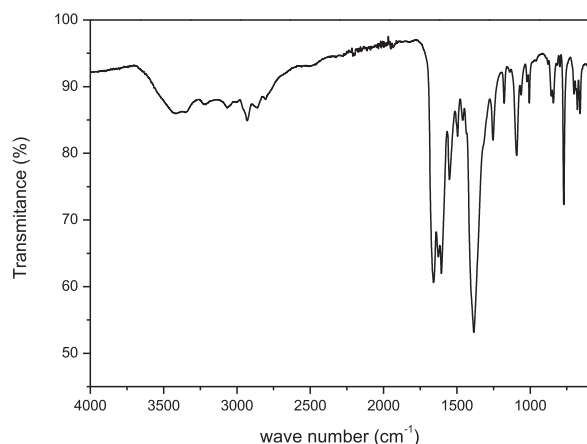
Fig. 3. IR spectra of Zn-URJC-13 material.
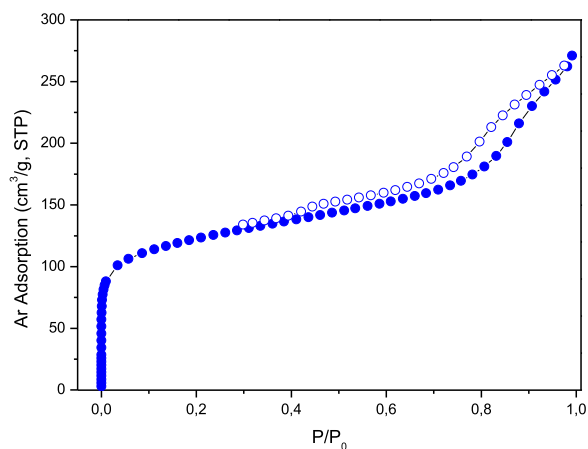
Fig. 4. Ar adsorption/desorption isotherms at 87 K of Zn-URJC-13.

by itself unable to continue the reaction (entry 2). When amount of catalyst was evaluated from 1 % to 2 % (entries 3–5), the epoxide conversion was almost total for 1.5 % of catalyst because the Zn concentration in the medium is higher, which favors the opening of epoxide's ring by means of interactions between epichlorohydrin and Zn. However, when amount of catalyst was increased to 2 % the conversion reaction decreased to 88 % due to the medium became saturated, making more difficult the reaction species diffusion, as it has been shown in other studies [18]. Besides when amount of co-catalyst was decreased to 4 % (entry 6), the reaction yield was 86 %, lower than 98 % for 5 % and 6 % (entry 7). This fact can be explained due to the increase the amount of co-catalyst, the concentration of bromide ions is higher, favoring the reaction, as it has been explained above. When pressure was evaluated at 12, 6 and 1 bar (entries 4, 8 and 9) the conversion was significantly decreased, since higher pressures boost the solubilization of carbon dioxide in the epoxide. And finally, the reaction yield was favored for longer reaction times (24 h, entre 4) at room temperature,

being decreased to almost the half when time was cut at 12 h or 6 h (entry 10 and 11), as it has been reported in literature [33,34].

This new Zn-based MOF material was compared to homogeneous and heterogeneous zinc from two different salts under the best reaction conditions obtained in the present work (Table 2). Using zinc nitrate, an epichlorohydrin conversion of 80 % was achieved, but with the intrinsic handicap of the catalyst recovery. On the other hand, the zinc bromide only achieved a conversion of 33 % acting in heterogeneous phase since was not soluble in the reaction conditions. These results demonstrate the catalytic activity of the heterogeneous Zn-URJC-13 and the importance of containing acid and basic sites in the same structure, with the clear advantage of the recover and reutilization of the MOF catalyst.

Based on the great results achieved in the cycloaddition reaction between CO_2 and epichlorohydrin obtained by the new MOF material Zn-URJC-13, different epoxides were evaluated as substrate under the reaction conditions of 1 mmol epoxide, 1.5 mol % catalyst, 5 mol % co-catalyst, 12 bar of CO_2, room temperature and 24 h of reaction time. The
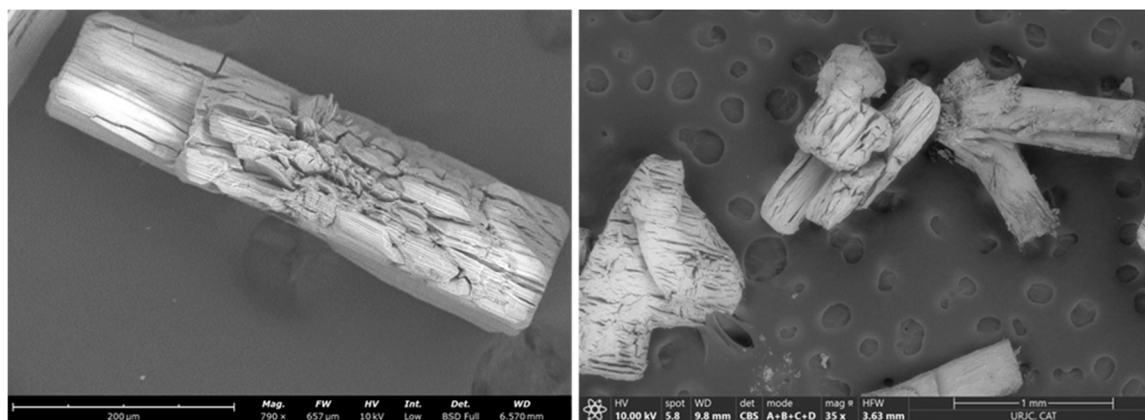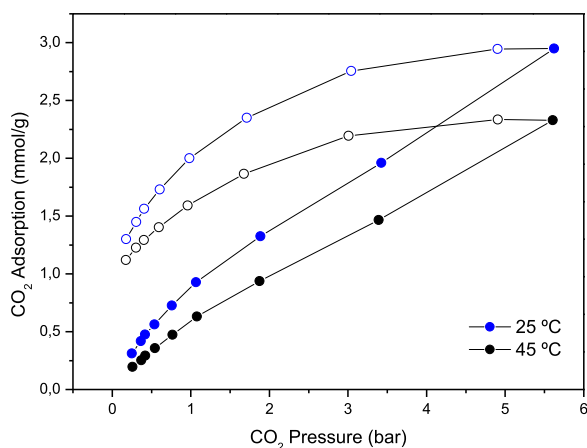
Fig. 5. SEM imagens of Zn-URJC-13.

Fig. 6. CO_2 adsorption/desorption isotherms of Zn-URJC-13.

Table 2
Reaction results obtained by different catalyst of zinc (II).

Catalyst	Conversion (%)[a]	Selectivity (%)[b]
$Zn(NO_3)_2$	80	
$ZnBr_2$	33	>99
Zn-URJC-13	98	

[a,b]Determinated by H NMR.

reaction results in terms of epoxide conversion and selectivity are summarized in Table 3. The epoxides used in the present work were propylene oxide, epichlorohydrin, 3,3-dimethyl-1,2-epoxybutane, 1,2-epoxipentane, allyl glycidyl ether, styrene oxide, 1,2-epoxitetradecane.

The reaction results are shown in Table 1, where it is evidenced that the epoxides with linear alkyl chain showed excellent results in epoxide conversion. As the chain length increases the reaction conversion slightly decreases from 99 % for propylene oxide (R= -CH_3) to 94 % for 1,2-epoxypentane (R= -$(CH_2)_2$-CH_3) (entry 4). However, for 1,2-epoxytetradecane (R= -$(CH_2)_{11}$-CH_3) (entry 7) the conversion drops considerably due to the large chain length, which can generate diffusional problems within the cavities of the material, thus reducing the reaction yield.

In addition, it was found that an increase in the volume of the epoxide substituent reduces the conversion of the reaction. In the case of epichlorohydrin (R= -CH_2Cl) (entry 2) the conversion was 98 %, since the small size of this molecule favors its diffusion through the channels of Zn-URJC-13, resulting in a high reaction yield. When 3,3-dimethyl-1,2-epoxybutane was used as substrate (entry 3), the reaction conversion decreased to 88 % (R= -$C(CH_3)_3$) due to the partial steric hindrance and/

or hydrophobicity shown by the tert-butyl group. When styrene oxide was used as a substrate (entry 6), the conversion of the epoxide decreased to 84 % because of the larger volume of the aromatic ring, which may not only generate higher steric hindrances of CO_2 to intact with the active sites and reducing the diffusion of the products through the channels of the material, but also the aromatic substituent may generate hydrophobicity inside the cavities. Despite this effect, the results attained for Zn-URJC-13 using styrene oxide are superior to those reported in the literature for other MOF materials so far, as it is shown in Table 4.
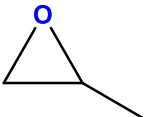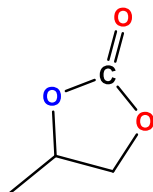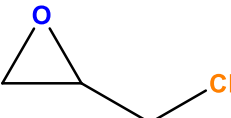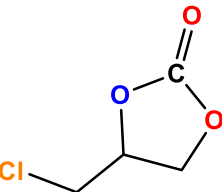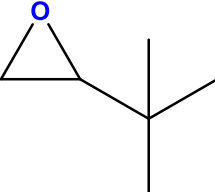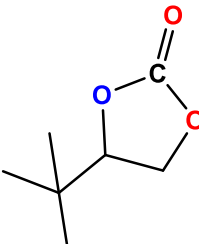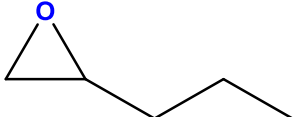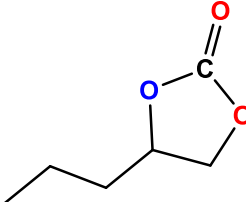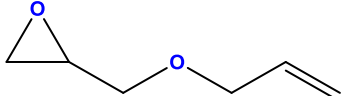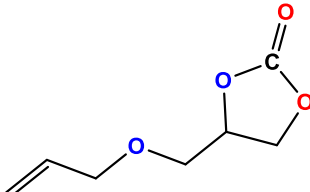
However, in the case of styrene oxide, the selectivity of the reaction is not total to cyclic carbonates, showing a value of 91 %, due to the formation of a dimer (Fig. 7). The formation of the dimer (2,5-diphenyl-1,4-dioxane) from the undesired dimerization reaction when styrene oxide was used, was unequivocally detected by H-NRM analysis (Fig. S4.17), which spectrum is included in Supporting information with the corresponding signals well identified. This dimer was also observed in previous works about CO_2 cycloaddition reaction using this epoxide [17,42].

Finally, the recyclability of this new Zn-URJC-13 material was evaluated in CO_2 cycloaddition reaction under the same reaction conditions using epichlorohydrin as substrate. The material was centrifugated to separate it from the reaction medium, washed tree times with $CHCl_3$ and dried under vacuum for 3 h. The reaction results obtain indicated that this material was stable in this reaction because of different reasons: i) the epoxide conversion kept almost constant (from 98 % to 95 % after the fifth reaction cycle) as shown in Fig. 8, ii) the XRD pattern was very similar to the fresh material (Fig. S5.6), and there is no presence of zinc metal ion in the reaction media, measured by ICP analysis. The slight drop in the epoxide conversion is due to a partial retention of the product inside the MOF's cavities, which was evidenced in the TGA analysis (Fig. S5.7) where a new mass loss was detected at 220 °C, also observed in other works [18].

3.3. Proposed reaction mechanism

The possible reaction mechanism for cycloaddition reaction between epichlorohydrin and CO_2 catalyzed by Zn-URJC-13 is depicted in Fig. 9, and it was developed basing on a previously mechanism reported in literature using epichlorohydrin as substrate [17,18,36,43]. In the first step the epichlorohydrin molecule interacts with the zinc metal center through the oxygen atom. This interaction produces the polarization of oxygen-carbon bond favoring the nucleophilic attack of bromide ion from TBAB, producing the opening of epoxide ring. In the second step, the CO_2 molecule interacts with amine group of 2-aminopiridine-4-carboxilic acid, giving rise to the nucleophilic attack of one oxygen atom from carbon dioxide molecule to the carbon atom from the carbon-bromide bonding of the intermediate, formed in first step. In the third step, the removal of bromide ion takes place, releasing it to the

Table 3
Reaction results for the different epoxides used in the cycloaddition reaction.

Entry	Epoxide	Carbonate	Conv. (%)[a]	Select. (%)[b]
1			99	99
2			98	99
3			88	99
4			94	99
5			96	99

Table 3 (*continued*)
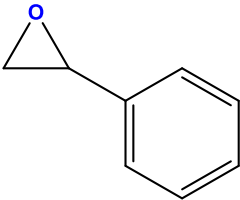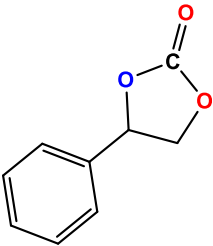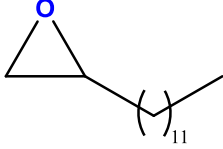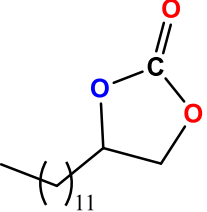
Entry	Epoxide	Carbonate	Conv. (%)[a]	Select. (%)[b]
6			84	90
7			57	99

Table 4
Other MOF materials in cycloaddition reaction between CO_2 and styrene oxide.

| Material	Conversion (%)	Reaction conditions				Ref.
		P (bar)	T (°C)	t (h)	Co-cat. (%)	
Zn-URJC-13	84	12	R.T.	24	5	This work
JLU-Liu22	65	1	80	48	5	[35]
Zn(Py)(Atz)	63	15	100	4	1	[36]
Zn-URJC-8	54	12	R.T.	24	5	[19]
Cu-URJC-8	49	12	R.T.	24	4	[18]
ZIF-8	11	20	100	4	-	[37]
MIL-101	63	20	100	4	-	[37]
CuBTC	48	20	100	4	-	[37]
IRMOF-3	33	20	100	4	-	[37]
Co-MOF-74	38	20	60	4	-	[38]
PCN-777-Hf	57	1	R.T.	48	10	[39]
MOF-808-Zr	26	1	R.T.	48	10	[40]
MOF-808-Hf	21	1	R.T.	48	10	[40]
MOF-1	58	1	50	48	2	[41]
MOF-2	65	1	50	48	2	[41]
MOF-3	65	1	50	48	2	[41]
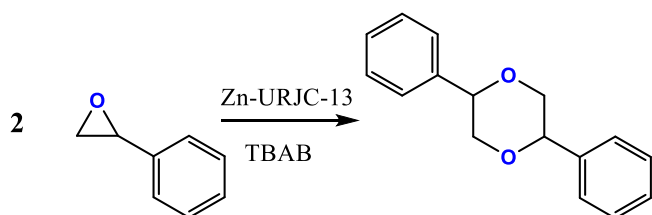
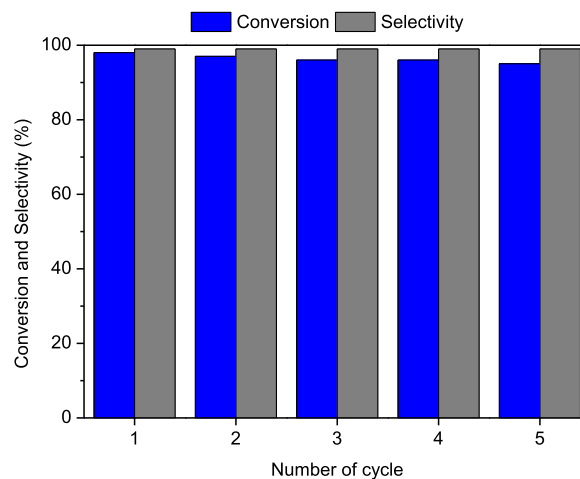**Fig. 7.** Secondary reaction of cyclodimerization of styrene oxide.

Fig. 8. Reusability of Zn-URJC-13 material after five consecutive cycles.

reaction medium and generating the formation of a second reaction intermediate. Finally in the fourth step, the oxygen atom from epoxide nucleophilic attacks the carbon atom of CO_2 molecule, closing the cycle and forming the cyclic carbonate, as well as leaving the catalyst regenerated.

4. Conclusions

The synthesis of a novel Metal-Organic Framework (MOF) material, named Zn-URJC-13, was reported for the first time. This MOF material was found to be suitable for CO_2 cycloaddition reactions with epoxides even bulky because it contains Zn and -NH2 groups which act as acid and basic Lewis sites and it shows permanent porosity with a bimodal porous system centered at 11 and 17 Å. Zn-URJC-13 catalyst was chemically stable in various common organic solvents and exhibited high affinity to CO_2 molecules, with a Q_{st} of 62 kJ/mol. The Zn-URJC-13 catalyst has demonstrated efficient performance in CO_2 cycloaddition reactions
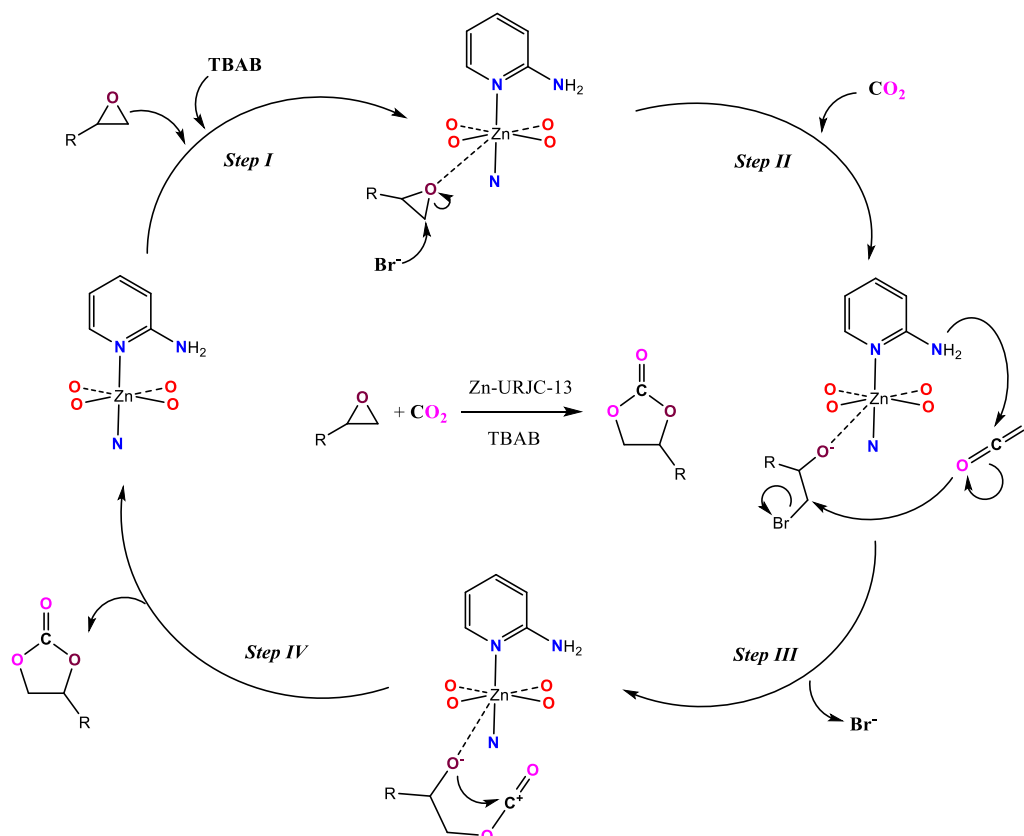
Fig. 9. Proposed mechanism for cycloaddition reaction between epichlorohydrin and CO_2 catalyzed by Zn-URJC-13.

using a wide range of epoxides, including those with long-chain or bulky substituents such as allyl glycidyl ether and styrene oxide. It achieves high epoxide conversion rates (above 84 %) and selectivity to carbonate products (above 90 %). When compared to other Zn-based MOF materials with similar or different structures but without amino groups, the new material outperformed them significantly. Zn-URJC-13 has been successfully reused in five consecutive reaction cycles, maintaining its efficient catalytic behavior and crystalline structure. The novel Zn-URJC-13 MOF combines structural features such as the presence of Zn, -NH2, hydrophobic pyridine, and suitable textural properties, which synergistically enhance the catalytic performance in CO_2 cycloaddition reactions with epoxides, making it a real alternative for industrial application.

CRediT authorship contribution statement

Jesús Tapiador: Investigation, Writing - Original Draft. Pedro Leo: Conceptualization, Methodology. Guillermo Calleja: Supervision. Gisela Orcajo: Supervision, Writing - Review & Editing, Conceptualization, Methodology, Funding acquisition.

Declaration of Competing Interest

The authors declare that they have no known competing financial interests or personal relationships that could have appeared to influence the work reported in this paper.

Data Availability

The data is not confidential.

Acknowledgements

Appendix A. Supporting information

Supplementary data associated with this article can be found in the online version at doi:10.1016/j.cattod.2023.114442.

References

[1] international energy agency, CO2 Emissions in 2022, 2022. ⟨www.iea.org⟩.
[2] A.A. Olajire, Valorization of greenhouse carbon dioxide emissions into value-added products by catalytic processes, J. CO₂ Util. 3–4 (2013) 74–92, https://doi.org/10.1016/j.jcou.2013.10.004.
[3] J.K. Heffernan, K. Valgepea, R. de Souza Pinto Lemgruber, I. Casini, M. Plan, R. Tappel, S.D. Simpson, M. Köpke, L.K. Nielsen, E. Marcellin, Enhancing CO₂-valorization using clostridium autoethanogenum for sustainable fuel and chemicals production, Front Bioeng. Biotechnol. 8 (2020), https://doi.org/10.3389/fbioe.2020.00204.
[4] J.A. Cecilia, D. Ballesteros Plata, E. Vilarrasa García, CO₂ valorization and its subsequent valorization, Molecules 26 (2021), https://doi.org/10.3390/molecules26020500.
[5] L. Fu, Z. Ren, W. Si, Q. Ma, W. Huang, K. Liao, Z. Huang, Y. Wang, J. Li, P. Xu, Research progress on CO₂ capture and utilization technology, J. CO₂ Util. 66 (2022), 102260, https://doi.org/10.1016/j.jcou.2022.102260.
[6] P. Gabrielli, M. Gazzani, M. Mazzotti, The role of carbon capture and utilization, carbon capture and storage, and biomass to enable a net-zero-CO₂ emissions chemical industry, Ind. Eng. Chem. Res. 59 (2020) 7033–7045, https://doi.org/10.1021/acs.iecr.9b06579.
[7] P.P. Pescarmona, Cyclic carbonates synthesised from CO₂: applications, challenges and recent research trends, Curr. Opin. Green. Sustain Chem. 29 (2021), 100457, https://doi.org/10.1016/j.cogsc.2021.100457.
[8] F. Nakibuule, S.A. Nyanzi, I. Oshchapovsky, O.F. Wendt, E. Tebandeke, Synthesis of cyclic carbonates from epoxides and carbon dioxide catalyzed by talc and other

phyllosilicates, BMC Chem. 14 (2020) 61, https://doi.org/10.1186/s13065-020-00713-2.

[9] P. Rollin, L.K. Soares, A.M. Barcellos, D.R. Araujo, E.J. Lenardão, R.G. Jacob, G. Perin, Five-membered cyclic carbonates: versatility for applications in organic synthesis, pharmaceutical, and materials sciences, Appl. Sci. 11 (2021), https://doi.org/10.3390/app11115024.

[10] V.F. Yusuf, N.I. Malek, S.K. Kailasa, Review on metal–organic framework classification, synthetic approaches, and influencing factors: applications in energy, drug delivery, and wastewater treatment, ACS Omega 7 (2022) 44507–44531, https://doi.org/10.1021/acsomega.2c05310.

[11] F.N. Al-Rowaili, U. Zahid, S. Onaizi, M. Khaled, A. Jamal, E.M. AL-Mutairi, A review for Metal-Organic Frameworks (MOFs) utilization in capture and conversion of carbon dioxide into valuable products, J. CO₂ Util. 53 (2021), 101715, https://doi.org/10.1016/j.jcou.2021.101715.

[12] M. Usman, N. Iqbal, T. Noor, N. Zaman, A. Asghar, M.M. Abdelnaby, A. Galadima, A. Helal, Advanced strategies in metal-organic frameworks for CO₂ capture and separation, Chem. Rec. 22 (2022), e202100230, https://doi.org/10.1002/tcr.202100230.

[13] W.G. Cui, G.Y. Zhang, T.L. Hu, X.H. Bu, Metal-organic framework-based heterogeneous catalysts for the conversion of C1 chemistry: CO, CO 2 and CH 4, Coord. Chem. Rev. 387 (2019) 79–120, https://doi.org/10.1016/j.ccr.2019.02.001.

[14] I. Campello, A. Sepúlveda-Escribano, E.V. Ramos-Fernández, Metal–Organic Frameworks (MOFs) for CO₂ Cycloaddition Reactions, Eng. Solut. CO₂ Convers. (2021) 407–427, https://doi.org/10.1002/9783527346523.ch17.

[15] T.K. Pal, D. De, P.K. Bharadwaj, Metal–organic frameworks for the chemical fixation of CO₂ into cyclic carbonates, Coord. Chem. Rev. 408 (2020), 213173, https://doi.org/10.1016/j.ccr.2019.213173.

[16] J. Liang, Y.B. Huang, R. Cao, Metal–organic frameworks and porous organic polymers for sustainable fixation of carbon dioxide into cyclic carbonates, Coord. Chem. Rev. 378 (2019) 32–65, https://doi.org/10.1016/j.ccr.2017.11.013.

[17] J. Tapiador, E. García-Rojas, P. López-Patón, G. Calleja, G. Orcajo, C. Martos, P. Leo, Influence of divalent metal ions on CO₂ valorization at room temperature by isostructural MOF-74 materials, J. Environ. Chem. Eng. 11 (2023), https://doi.org/10.1016/j.jece.2023.109497.

[18] J. Tapiador, P. Leo, F. Gándara, G. Calleja, G. Orcajo, Robust Cu-URJC-8 with mixed ligands for mild CO₂ cycloaddition reaction, J. CO₂ Util. 64 (2022), 102166, https://doi.org/10.1016/j.jcou.2022.102166.

[19] J. Tapiador, P. Leo, A. Rodríguez-Diéguez, D. Choquesillo-Lazarte, G. Calleja, G. Orcajo, A novel Zn-based-MOF for efficient CO₂ adsorption and conversion under mild conditions, Catal. Today 390-391 (2022) 230–236, https://doi.org/10.1016/j.cattod.2021.11.025.

[20] W.Y. Gao, Y. Chen, Y. Niu, K. Williams, L. Cash, P.J. Perez, L. Wojtas, J. Cai, Y. S. Chen, S. Ma, Crystal engineering of an nbo topology metal-organic framework for chemical fixation of CO₂ under ambient conditions, Angew. Chem. - Int. Ed. 53 (2014) 2615–2619, https://doi.org/10.1002/anie.201309778.

[21] Z.X. Bian, Y.Z. Zhang, D. Tian, X. Zhang, L.H. Xie, M. Zhao, Y. Xie, J.R. Li, Co7-cluster-based metal-organic frameworks with mixed carboxylate and pyrazolate ligands: construction and CO2 adsorption and fixation, Cryst. Growth Des. 20 (2020) 7972–7978, https://doi.org/10.1021/acs.cgd.0c01232.

[22] A.C. Kathalikkattil, Y. Gu, J.F. Kurisingal, H. Lee, H. Kim, Y. Choe, D.W. Park, A catalytic approach of blending CO₂-activating MOF struts for cycloaddition reaction in a helically interlaced Cu(II) amino acid imidazolate framework: DFT-corroborated investigation, Res. Chem. Intermed. 47 (2021) 3979–3997, https://doi.org/10.1007/s11164-021-04507-6.

[23] S.S. Dhankhar, C.M. Nagaraja, Construction of 3D lanthanide based MOFs with pores decorated with basic imidazole groups for selective capture and chemical fixation of CO₂, N. J. Chem. 44 (2020) 9090–9096, https://doi.org/10.1039/d0nj01448f.

[24] J. Kim, S.N. Kim, H.G. Jang, G. Seo, W.S. Ahn, CO₂ cycloaddition of styrene oxide over MOF catalysts, Appl. Catal. A Gen. 453 (2013) 175–180, https://doi.org/10.1016/j.apcata.2012.12.018.

[25] S. Brunauer, P.H. Emmett, E. Teller, Adsorption of gases in multimolecular layers, J. Am. Chem. Soc. 60 (1938) 309–319, https://doi.org/10.1021/ja01269a023.

[26] M. Thommes, K. Kaneko, A.V. Neimark, J.P. Olivier, F. Rodriguez-Reinoso, J. Rouquerol, K.S.W. Sing, Physisorption of gases, with special reference to the evaluation of surface area and pore size distribution (IUPAC Technical Report), Pure Appl. Chem. 87 (2015) 1051–1069, https://doi.org/10.1515/pac-2014-1117.

[27] T. Ghanbari, F. Abnisa, W.M.A. Wan Daud, A review on production of metal organic frameworks (MOF) for CO₂ adsorption, Sci. Total Environ. 707 (2020), 135090, https://doi.org/10.1016/j.scitotenv.2019.135090.

[28] J.T. Culp, M.R. Smith, E. Bittner, B. Bockrath, Hysteresis in the physisorption of CO₂ and N2 in a flexible pillared layer nickel cyanide, J. Am. Chem. Soc. 130 (2008) 12427–12434, https://doi.org/10.1021/ja802474b.

[29] M. Abunowara, M.A. Bustam, S. Sufian, U. Eldemerdash, Description of carbon dioxide adsorption and desorption onto Malaysian coals under subcritical condition, Procedia Eng. 148 (2016) 600–608, https://doi.org/10.1016/j.proeng.2016.06.521.

[30] L. Yu, M. Kanezashi, H. Nagasawa, T. Tsuru, Role of amine type in CO₂ separation performance within amine functionalized silica/organosilica membranes: a review, Appl. Sci. 8 (2018), https://doi.org/10.3390/app8071032.

[31] S. Couck, J.F.M. Denayer, G.V. Baron, T. Rémy, J. Gascon, F. Kapteijn, An amine-functionalized MIL-53 metal-organic framework with large separation power for CO₂ and CH4, J. Am. Chem. Soc. 131 (2009) 6326–6327, https://doi.org/10.1021/ja900555r.

[32] N. Planas, A.L. Dzubak, R. Poloni, L.C. Lin, A. McManus, T.M. McDonald, J. B. Neaton, J.R. Long, B. Smit, L. Gagliardi, The mechanism of carbon dioxide adsorption in an alkylamine-functionalized metal-organic framework, J. Am. Chem. Soc. 135 (2013) 7402–7405, https://doi.org/10.1021/ja4004766.

[33] S.-L. Hou, J. Dong, B. Zhao, Formation of C□X bonds in CO₂ chemical fixation catalyzed by metal−organic frameworks, Adv. Mater. 32 (2020) 1806163, https://doi.org/10.1002/adma.201806163.

[34] H. He, J.A. Perman, G. Zhu, S. Ma, Metal-organic frameworks for CO₂ chemical transformations, Small 12 (2016) 6309–6324, https://doi.org/10.1002/smll.201602711.

[35] J. Gu, X. Sun, X. Liu, Y. Yuan, H. Shan, Y. Liu, Highly efficient synergistic CO2conversion with epoxide using copper polyhedron-based MOFs with Lewis acid and base sites, Inorg. Chem. Front 7 (2020) 4517–4526, https://doi.org/10.1039/d0qi00938e.

[36] J. Lan, Y. Qu, X. Zhang, H. Ma, P. Xu, J. Sun, A novel water-stable MOF Zn(Py)(Atz) as heterogeneous catalyst for chemical conversion of CO₂ with various epoxides under mild conditions, J. CO₂ Util. 35 (2020) 216–224, https://doi.org/10.1016/j.jcou.2019.09.019.

[37] J. Kim, S.-N. Kim, H.-G. Jang, G. Seo, W.-S. Ahn, CO₂ cycloaddition of styrene oxide over MOF catalysts, Appl. Catal. A Gen. 453 (2013) 175–180, https://doi.org/10.1016/j.apcata.2012.12.018.

[38] H.-Y. Cho, D.-A. Yang, J. Kim, S.-Y. Jeong, W.-S. Ahn, CO₂ adsorption and catalytic application of Co-MOF-74 synthesized by microwave heating, Catal. Today 185 (2012) 35–40, https://doi.org/10.1016/j.cattod.2011.08.019.

[39] L. Jin, Q. Qin, L. Dong, S. Liu, S. Xie, J. Lu, A. Xu, J. Liu, H. Liu, Y. Yao, X. Hou, M. Fan, Study of the cycloaddition of CO₂ with styrene oxide over six-connected spn topology MOFs (Zr, Hf) at room temperature, Chem. – A Eur. J. 27 (2021) 14947–14963, https://doi.org/10.1002/chem.202102408.

[40] L. Jin, Q. Qin, L. Dong, S. Liu, S. Xie, J. Lu, A. Xu, J. Liu, H. Liu, Y. Yao, X. Hou, M. Fan, Study of the cycloaddition of CO₂ with styrene oxide over six-connected spn topology MOFs (Zr, Hf) at room temperature, Chem. – A Eur. J. 27 (2021) 14947–14963, https://doi.org/10.1002/chem.202102408.

[41] H. Lin, C.H. Deng, X. Qiu, X. Liu, J.G. Ma, P. Cheng, Structural design of Mn-metal-organic frameworks toward highly efficient solvent-free cycloaddition of CO₂, Cryst. Growth Des. 21 (2021) 3728–3735, https://doi.org/10.1021/acs.cgd.1c00037.

[42] B. Mousavi, S. Chaemchuen, S. Phatanasri, C. Chen, C. Zeng, R. Ganguly, S. Zhuiykov, F. Verpoort, Selective cyclodimerization of epichlorohydrin to dioxane derivatives over MOFs, Arab. J. Chem. 13 (2020) 1088–1093, https://doi.org/10.1016/j.arabjc.2017.09.011.

[43] J. Tapiador, E. García-Rojas, P. Leo, C. Martos, G. Calleja, G. Orcajo, Copper MOFs performance in the cycloaddition reaction of CO₂ and epoxides, Microporous Mesoporous Mater. 361 (2023), 112741, https://doi.org/10.1016/j.micromeso.2023.112741.